

Special Issue: Polymers for Microelectronics

Guest Editors: Dr Brian Knapp (Promerus LLC) and
Prof. Paul A. Kohl (Georgia Institute of Technology)

EDITORIAL

Polymers for Microelectronics

B. Knapp and P. A. Kohl, *J. Appl. Polym. Sci.* 2014, DOI: [10.1002/app.41233](https://doi.org/10.1002/app.41233)

REVIEW

Negative differential conductance materials for flexible electronics

A. Nogaret, *J. Appl. Polym. Sci.* 2014, DOI: [10.1002/app.40169](https://doi.org/10.1002/app.40169)

RESEARCH ARTICLES

Generic roll-to-roll compatible method for insolubilizing and stabilizing conjugated active layers based on low energy electron irradiation

M. Helgesen, J. E. Carlé, J. Helt-Hansen, A. Miller, and F. C. Krebs, *J. Appl. Polym. Sci.* 2014, DOI: [10.1002/app.40795](https://doi.org/10.1002/app.40795)

Selective etching of polylactic acid in poly(styrene)-block-poly(D,L)lactide diblock copolymer for nanoscale patterning

C. Cummins, P. Mokarian-Tabari, J. D. Holmes, and M. A. Morris, *J. Appl. Polym. Sci.* 2014, DOI: [10.1002/app.40798](https://doi.org/10.1002/app.40798)

Preparation and dielectric behavior of polyvinylidene fluoride composite filled with modified graphite nanoplatelet

P. Xie, Y. Li, and J. Qiu, *J. Appl. Polym. Sci.* 2014, DOI: [10.1002/app.40229](https://doi.org/10.1002/app.40229)

Design of a nanostructured electromagnetic polyaniline–Keggin iron–clay composite modified electrochemical sensor for the nanomolar detection of ascorbic acid

R. V. Lilly, S. J. Devaki, R. K. Narayanan, and N. K. Sadanandhan, *J. Appl. Polym. Sci.* 2014, DOI: [10.1002/app.40936](https://doi.org/10.1002/app.40936)

Synthesis and characterization of novel phosphorous-silicone-nitrogen flame retardant and evaluation of its flame retardancy for epoxy thermosets

Z.-S. Li, J.-G. Liu, T. Song, D.-X. Shen, and S.-Y. Yang, *J. Appl. Polym. Sci.* 2014, DOI: [10.1002/app.40412](https://doi.org/10.1002/app.40412)

Electrical percolation behavior and electromagnetic shielding effectiveness of polyimide nanocomposites filled with carbon nanofibers

L. Nayak, T. K. Chaki, and D. Khastgir, *J. Appl. Polym. Sci.* 2014, DOI: [10.1002/app.40914](https://doi.org/10.1002/app.40914)

Morphological influence of carbon modifiers on the electromagnetic shielding of their linear low density polyethylene composites

B. S. Villacorta and A. A. Ogale, *J. Appl. Polym. Sci.* 2014, DOI: [10.1002/app.41055](https://doi.org/10.1002/app.41055)

Electrical and EMI shielding characterization of multiwalled carbon nanotube/polystyrene composites

V. K. Sachdev, S. Bhattacharya, K. Patel, S. K. Sharma, N. C. Mehra, and R. P. Tandon, *J. Appl. Polym. Sci.* 2014, DOI: [10.1002/app.40201](https://doi.org/10.1002/app.40201)

Anomalous water absorption by microelectronic encapsulants due to hygrothermal-induced degradation

M. van Soestbergen and A. Mavinkurve, *J. Appl. Polym. Sci.* 2014, DOI: [10.1002/app.41192](https://doi.org/10.1002/app.41192)

Design of cyanate ester/azomethine/ZrO₂ nanocomposites high-k dielectric materials by single step sol-gel approach

M. Ariraman, R. Sasi Kumar and M. Alagar, *J. Appl. Polym. Sci.* 2014, DOI: [10.1002/app.41097](https://doi.org/10.1002/app.41097)

Furan/imide Diels–Alder polymers as dielectric materials

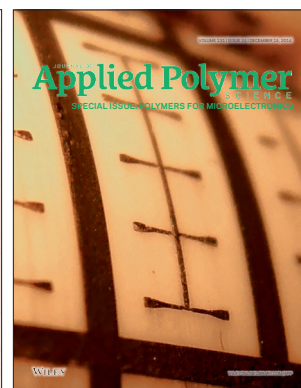
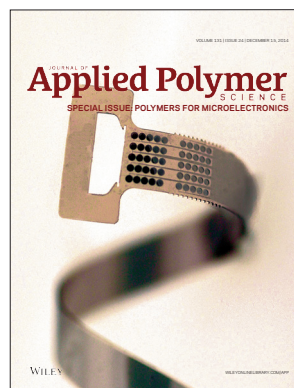
R. G. Lorenzini and G. A. Sotzing, *J. Appl. Polym. Sci.* 2014, DOI: [10.1002/app.40179](https://doi.org/10.1002/app.40179)

High dielectric constant polyimide derived from 5,5'-bis[(4-amino) phenoxy]-2,2'-bipyrimidine

X. Peng, Q. Wu, S. Jiang, M. Hanif, S. Chen, and H. Hou, *J. Appl. Polym. Sci.* 2014, DOI: [10.1002/app.40828](https://doi.org/10.1002/app.40828)

The influence of rigid and flexible monomers on the physical-chemical properties of polyimides

T. F. da Conceição and M. I. Felisberti, *J. Appl. Polym. Sci.* 2014, DOI: [10.1002/app.40351](https://doi.org/10.1002/app.40351)



Special Issue: Polymers for Microelectronics

Guest Editors: Dr Brian Knapp (Promerus LLC) and
Prof. Paul A. Kohl (Georgia Institute of Technology)

Development of polynorbornene as a structural material for microfluidics and flexible BioMEMS

A. E. Hess-Dunning, R. L. Smith, and C. A. Zorman, *J. Appl. Polym. Sci.* 2014, DOI: [10.1002/app.40969](https://doi.org/10.1002/app.40969)

A thin film encapsulation layer fabricated via initiated chemical vapor deposition and atomic layer deposition

B. J. Kim, D. H. Kim, S. Y. Kang, S. D. Ahn, and S. G. Im, *J. Appl. Polym. Sci.* 2014, DOI: [10.1002/app.40974](https://doi.org/10.1002/app.40974)

Surface relief gratings induced by pulsed laser irradiation in low glass-transition temperature azopolysiloxanes

V. Damian, E. Resmerita, I. Stoica, C. Ibanescu, L. Sacarescu, L. Rocha, and N. Hurduc, *J. Appl. Polym. Sci.* 2014, DOI: [10.1002/app.41015](https://doi.org/10.1002/app.41015)

Polymer-based route to ferroelectric lead strontium titanate thin films

M. Benkler, J. Hobmaier, U. Gleißner, A. Medesi, D. Hertkorn, and T. Hanemann, *J. Appl. Polym. Sci.* 2014, DOI: [10.1002/app.40901](https://doi.org/10.1002/app.40901)

The influence of dispersants that contain polyethylene oxide groups on the electrical resistivity of silver paste

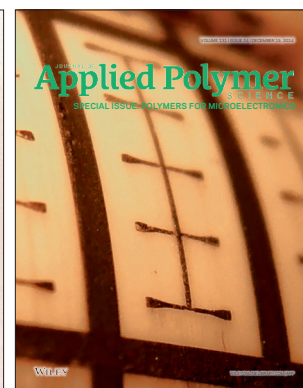
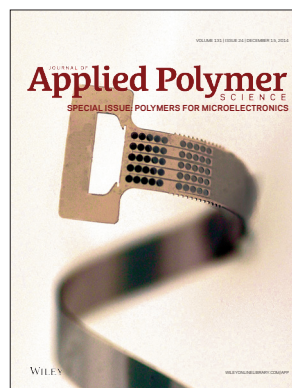
T. H. Chiang, Y.-F. Chen, Y. C. Lin, and E. Y. Chen, *J. Appl. Polym. Sci.* 2014, DOI: [10.1002/app.41183](https://doi.org/10.1002/app.41183)

Quantitative investigation of the adhesion strength between an SU-8 photoresist and a metal substrate by scratch tests

X. Zhang, L. Du, and M. Zhao, *J. Appl. Polym. Sci.* 2014, DOI: [10.1002/app.41108](https://doi.org/10.1002/app.41108)

Thermodynamic and kinetic aspects of defectivity in directed self-assembly of cylinder-forming diblock copolymers in laterally confining thin channels

B. Kim, N. Laachi, K. T. Delaney, M. Carilli, E. J. Kramer, and G. H. Fredrickson, *J. Appl. Polym. Sci.* 2014, DOI: [10.1002/app.40790](https://doi.org/10.1002/app.40790)



The Influence of Dispersants that Contain Polyethylene Oxide Groups on the Electrical Resistivity of Silver Paste

Tzu Hsuan Chiang,¹ Yi-Fu Chen,² Ya Chun Lin,¹ Emi Yun Chen¹

¹Department of Energy Engineering, National United University, Miaoli 36003, Taiwan, Republic of China

²Specialty Alloy Development Section, New Materials R & D Department, China Steel Corporation, 1, Chung Kang Road, Hsiao Kang, Kaohsiung 81233, Taiwan, Republic of China

Correspondence to: T. H. Chiang (E-mail: thchiang@nuu.edu.tw)

ABSTRACT: This study investigated the effects of dispersants on the electrical resistivity of silver pastes. The dispersants in the polyoxyethylene-*p*-(1,1,3,3-tetramethylbutyl) phenyl ethers system contain several polyethylene oxide (PEO) groups (m), which affect the viscosity and electrical resistivity of the silver pastes. The morphologies of the cured silver pastes for different dispersants and different content were obtained by scanning electronic microscopy. In this study, octylphenol ethylene oxide condensate, poly(oxyethylene) isooctylphenyl ether (X-100, the number of PEO groups was $m = 9.5$) has excellent ability to disperse silver particles. A loading of 75 wt % of silver powder was used to prepare silver paste that contained 0.8 wt % of X-100. This paste had the lowest viscosity and the lowest electrical resistivity of cured silver paste on the indium tin oxide (ITO) film and ITO glass, i.e., 5.52×10^{-5} and $6.82 \times 10^{-5} \Omega \text{ cm}$. © 2014 Wiley Periodicals, Inc. *J. Appl. Polym. Sci.* **2014**, *131*, 41183.

KEYWORDS: composites; properties and characterization; surfactants; viscosity and viscoelasticity

Received 20 May 2014; accepted 29 June 2014

DOI: 10.1002/app.41183

INTRODUCTION

In recent years, highly conductive silver pastes have been used extensively in industry as electrodes in various products, i.e., solar cells,^{1,2} light emitting diodes (LEDs),³ flat panel displays,⁴ touch panels,⁵ capacitors,⁶ and dye-sensitized solar cells.⁷ The electrode was obtained very rapidly by conductive silver pastes using screen printing through a patterned screen mask, and the cured silver pastes had low electrical resistivity. A high-performance, high-quality silver paste should provide several beneficial features, such as good printability, fine line and high aspect ratio, long screen life, solderability, and good electrical and mechanical properties, including high adhesion and reliability.

Most silver paste-based, conductive formulations have very high silver particle loadings, i.e., 70–85 wt %. The use of high silver particle loading in polymers can result in high viscosity and poor dispensability of conductive pastes, causing the cured silver pastes to have poor conductivity and poor adhesion for some substances. Also, a significant amount of silver powder is consumed, which increases the cost of the conductive paste. Therefore, the kind and amount of dispersant are very important considerations because of their potential effects on the homogeneity of the silver particles in the polymer. The desirable conditions are a high concentration of silver particles with low

viscosity in order to help prevent the agglomeration of the silver particles in the polymer.

In this study, we used polyoxyethylene-*p*-(1,1,3,3-tetramethylbutyl) phenyl ethers (Triton X system) surfactants as dispersants for the silver particles. The Triton X system incorporates non-ionic surfactants with both a hydrophilic polyethylene oxide group and hydrophobic hydrocarbon groups as *p*-(1,1,3,3-tetramethylbutyl)-phenyl. The Triton X system's surfactants possess several important characteristics, including wetting, detergency, superior hard surface, stabilization of coatings, metal cleaning, and excellent emulsification performance, and they are offered in a range of hydrophilic-lipophilic balances (HLBs) to match specific wetting and dispersing requirements.⁸ They are important ingredients of primary emulsifier mixtures used in the manufacture of emulsion polymers and stabilizers in latex polymers. Therefore, the Triton X system's surfactants can be applied extensively in various fields. For example, poly(oxyethylene) isooctylphenyl ether (X-100) dispersant usually is used to disperse inorganic powders, e.g., nano lead zirconate titanate (PZT) powder,⁹ barium titanate nano powder (BaTiO_3),¹⁰ yttrium oxide/zirconium oxide ($\text{Y}_2\text{O}_3/\text{ZrO}_2$) powders,¹¹ slurries,¹² multiwall carbon nanotubes (MWCNTs),^{13–17} single-walled carbon nanotubes (SWNTs),^{18,19} and nanocrystal indium tin oxide (ITO) particles.²⁰ Other dispersants, such as *tert*-

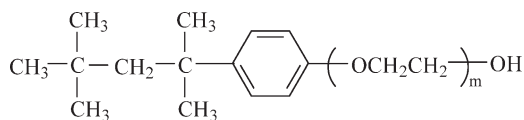


Figure 1. Structure of polyoxyethylene-*p*-(1,1,3,3-tetramethylbutyl) phenyl ethers.

octylphenoxy poly(ethoxyethanol) (X-114), also are used to disperse ZrO_2 particles,²⁰ yttria-stabilized zirconia (TZ-3Y) powders,²¹ and phosphor.²² X-100 also is used in the field of biotechnology, such as its use in the separation of protein from cell membranes²³ and extracting DNA.²⁴ In addition, the Triton X system's surfactants have polyethylene oxide groups that are used to stabilize the nanoparticles.²⁵ Due to the steric stabilization of these particles in nonpolar solvents, van der Waals attractions are substantially screened and a steep steric repulsion is introduced between the particles at contact, which avoids agglomeration.²⁶

In this study, we used saturated polyester resin as the polymer matrix because of its excellent properties of mechanical, chemical, and electrical stability. It also has excellent flexibility strength, which makes it useful as an electrical conducting material in the form of flexible substrates. The electrodes of a touch panel usually are prepared by screen printing the silver paste on to an ITO film or an ITO glass. In addition, we found that Triton X dispersants had not yet been used to disperse silver particles. Therefore, the aims of this study were to determine how to prepare silver paste and to investigate the effects of the cured silver pastes on the electrical resistivity when different contents of Triton X dispersants were used.

EXPERIMENTAL

The silver powder was supplied by Thin Tech Materials Technology, Taiwan. The average particle size (D_{av}) was 2.14 μm , the tap density was 5.54 g cm^{-3} , the mass–median–diameter (D_{50}) was 1.87 μm , specific surface area was 0.68 $\text{m}^2 \text{g}^{-1}$, and the

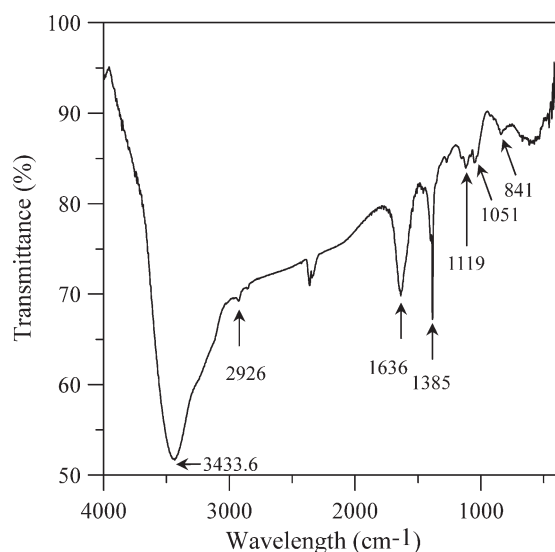


Figure 2. FTIR spectrum of silver particles.

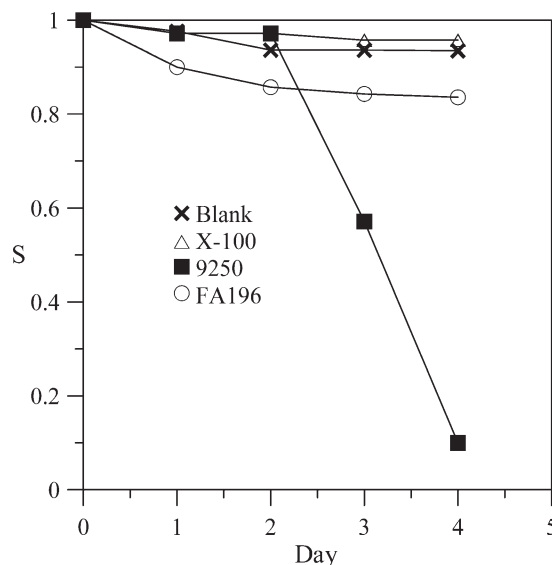


Figure 3. Sedimentation behavior of different types of dispersants.

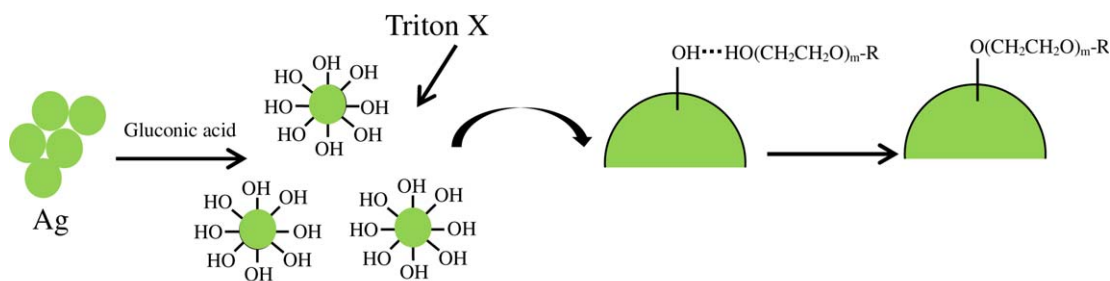
powder contained 0.6% of gluconic acid to protect the silver particles from being oxidized.

The sheet resistance of the ITO film was $600 \pm 100 \Omega/\square$, and its thickness was $197 \pm 20 \mu\text{m}$. The sheet resistance of the ITO glass was $500 \Omega/\square$, and its thickness was 1.1 mm, including an ITO coating that ranged in thickness from 200 to 400 nm. These products were purchased from EFUN Technology, Taiwan, and Uni-onward, Taiwan, respectively. The saturated polyester resin (ES-100) was provided by Chia Chung, and its solids content with 30% in the *n*-butyl glycidyl ether solvent. Trixene BI 7960 as hardness was a blocked isocyanate based on hexamethylene diisocyanate (HDI) biuret. The dibutyltin dilaurate (DBTDL), which was used as an accelerating agent, was supplied by An Fong Development, Taiwan. The *n*-butyl glycidyl ether solvent was provided by ACR Tech, Taiwan. Disponer 9250 (solution of a copolymer with acidic groups) and NUOSPERSE[®] FA196 (anionic dispersant) were supplied by Elementis Specialties, Taiwan.

The Triton X dispersants consisted of polyoxyethylene-*p*-(1,1,3,3-tetramethylbutyl) phenyl ethers, as shown in Figure 1, and they had different numbers of PEO groups (m). In this study, we used various dispersants, such as 4-(1,1,3,3-tetramethylbutyl)phenyl-polyethylene glycol, polyethylene glycol 4-*tert*-octylphenyl ether, (X-45, $m = 4.5$); *tert*-octylphenoxy poly(ethoxyethanol), (X-114, $m = 7.5$); octylphenol ethylene oxide condensate, poly(oxyethylene) isooctylphenyl ether, (X-100, $m = 9.5$); octylphenol ethoxylate, (X-165, $m = 16$); 2-[4-(2,4,4-trimethylpentan-2-yl) phenoxy] ethanol, (X-305, $m = 30$); and polyethylene glycol *tert*-octylphenyl ether (X-405, $m = 35$). All of the dispersants were purchased from Dow Chemical Company.

Preparation of Silver Paste

The silver paste was prepared by using 24.2 wt % of resin solution (containing 100 g of ES-100, 20 g of BI7960, and 0.13 g of DBTDL) and 0.8 wt % of various types of dispersants. The mixtures were stirred for 1 h and then 75 wt % of silver powder and 4 mL of *n*-butyl glycidyl ether were added via five millings in a milling process using a triple-roller mill (EXAKT,



R: (p-(1,1,3,3-tetramethylbutyl)-phenyl) groups

Figure 4. Schematic illustration of Triton X system surfactants being absorbed on silver particles. [Color figure can be viewed in the online issue, which is available at wileyonlinelibrary.com.]

Germany) to form conductive silver paste. The curing of all silver pastes was conducted at 140°C for 40 min. The conductive films were formed after heating.

Analysis of the Characteristics of Silver Paste

The silver paste was printed using a 400-mesh, stainless-steel screen with an emulsion buildup (thickness of 12 μm) mounted on a frame that measured 24.3 × 29.7 cm. The pattern area measured 1.5 × 2 cm. The pattern was printed in the forward direction only using a squeegee that had a durometer hardness of 80. The pattern was used to measure the electrical resistivity of the cured silver pastes using a four-point probe instrument manufactured by Ever Beig International Corporation. The electrical resistivity, ρ , was calculated as follows:

$$\rho = 4.532t \frac{V}{I},$$

where t is the thickness of the film, V is the voltage, and I is the DC electric current supplied by a power supply (Tektronix, DMM40506-1/2 Digit Precision Multimeter). The microstructures of the cured silver pastes were observed by JEOL JED 2300 field emission scanning electronic microscopy (SEM). The viscosities of the silver pastes were measured by a rheometer (Kinexus Pro) from Malvern. The experiments were conducted

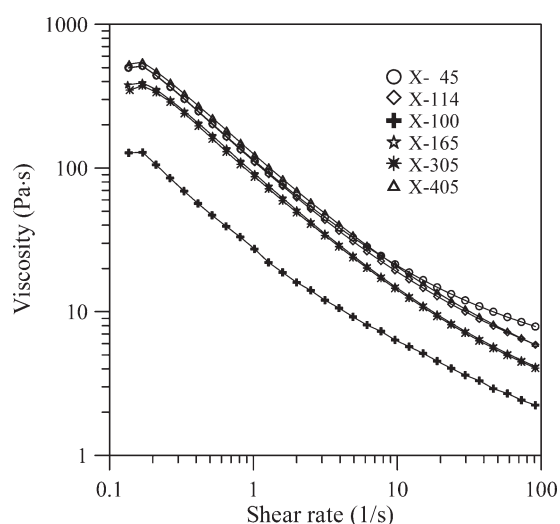


Figure 5. Viscosity of different m of Triton X dispersants.

with a cone and plate geometry (diameter: 40 mm; angle: 4°; truncation: 54 μm).

The sedimentation behavior was examined for all suspensions that contained different types of dispersants.²⁵ A 10 g of ES-100 resin was mixed with 0.3 g of various dispersants and 0.2 g of silver powder, and the mixture was poured into a 10-mL graduated cylinder. The mixture was allowed to stand for some time, and the height of the precipitate was observed during the standing time. First, the initial suspension height (h_0) and the sedimentation height (h) after different times were measured. The sedimentation coefficient for each sample was calculated using the equation $S = h/h_0$.

RESULTS AND DISCUSSION

Effect of Dispersant Types on Sedimentation Behavior

The sedimentation coefficient (S value) of sedimentation behavior indicates the powder's characteristics with respect to the formation of well-dispersed, highly stable suspensions. This information helped us eliminate dispersants that did a poor job of dispersing the silver particles. In this study, the silver particles contained 0.6% of gluconic acid to protect the silver particles from being oxidized. Figure 2 shows the FTIR spectra that were recorded for the silver particles. The peak at 3433.6 cm^{-1} was very broad and strong, and it was assigned to the hydroxyl group (–OH), either from the gluconic acid, adsorbed moisture, or both. The peak at 2926 cm^{-1} was due to the aliphatic C–H stretching; the peak at 1636 cm^{-1} was assigned to the δ (O–H) bending of water; the peak at 1385 cm^{-1} was due to C–H bending vibrations; and the peak at 1119 cm^{-1} corresponded to the –C–O–C stretching vibration in the glucose bonds. The band at 1051 cm^{-1} was attributed to C–O stretching in the C–OH groups of the gluconic acid, indicating that gluconic acid was contained in the silver particles; the band at 841 cm^{-1} was attributed to the stretching vibrations of the entire glucose ring. The gluconic acid was bound to the surfaces of the particulate silver atoms through its oxygen atoms.²⁷ The coordination of the oxygen atoms of the gluconic acid to the silver particles allows for a particle that has more stable functional hydroxyl groups.²⁸

Figure 3 shows how the different types of dispersants affected the sedimentation behavior of the silver particles. Figure 3

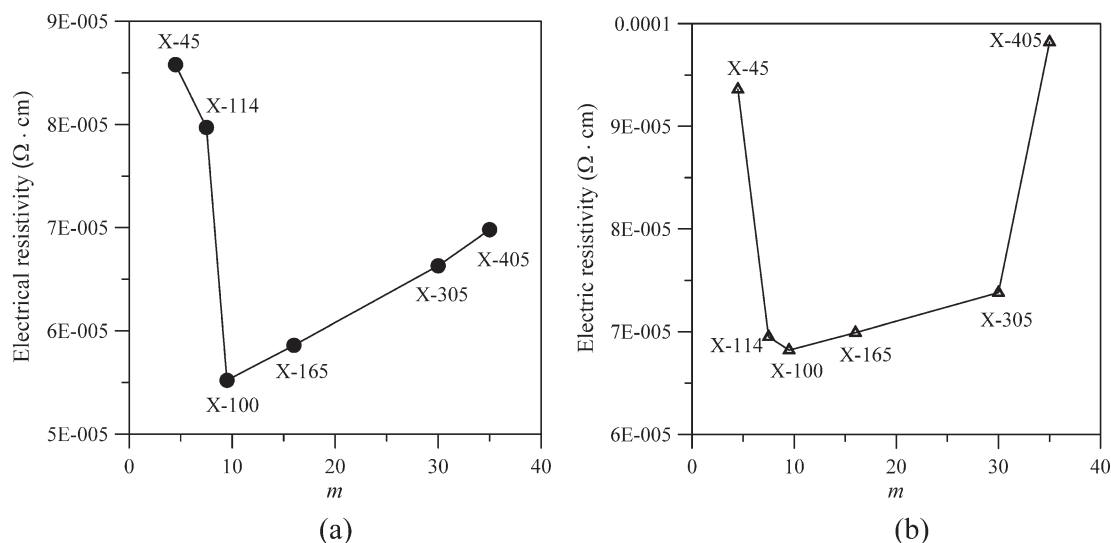


Figure 6. Electrical resistivity of different Triton X dispersants: (a) ITO film; (b) ITO glass.

presents data for the following combinations: 2.0 wt % of silver powder mixed with 3.0 wt % of Disponer 9250; 3.0 wt % of anionic dispersant FA196; and 3.0 wt % of nonionic dispersant X-100 in 95.0 wt % of ES-100. The results indicated that the silver particles made with X-100 dispersant had the highest *S* value, followed by the silver particles made without dispersant (blank). Based on the sedimentation experiments that lasted 4 days, the silver particles that were made using Disponer 9250 and FA196 had an *S* value that was lower than that of the blank which means that the silver particles produced agglomeration. The major reason the blank had a good *S* value was the 0.6% of gluconic acid that was coated on the silver particles, providing a part of the steric stabilization between the silver particles,²⁹ allowing them form a good dispersion in the resin. Disponer 9250 is a copolymer solution with acidic groups that easily produced flocculation to contain hydroxyl groups on the silver particles. The anionic dispersant FA196 has poorer dispersion of the silver particles than X-100 in the polyester. A major reason for this was that the anionic dispersant FA196 produces a negative charge that cannot form steric stabilization for the silver particles. However, X-100 can form steric stabilization for the silver particles. Since the silver particles contained 0.6% of gluconic acid to protect the silver particles from being oxidized, the surfaces of the silver particles were hydrophilic. The interaction between the hydrophilic hydroxyl groups on the silver particles and the hydrophilic PEO groups of X-100 dispersant is a contribution from its hydroxyl end-groups, which probably occurs by anchoring through the etherification³⁰ reacted on silver particles, owing to the formation of ether,³¹ as shown in Figure 4. The hydrophobic hydrocarbon (*p*-(1,1,3,3-tetramethylbutyl)phenyl) groups facing the polyester make the original hydrophilic surface of the silver particles become hydrophobic as the moiety stabilizes the silver particles, providing effective steric stabilization to overcome the large van der Waals forces among the silver particles, thereby improving their dispersion effect.

As a result, the interfacial tension between the silver particles and polyester is reduced, which separates the silver particles

from the polyester and hinders association of the silver particles. The hydrophilic PEO groups in the silver paste that are adsorbed on the surfaces of the silver particles form a brush-like layer and generate steric hindrance among the silver particles, making them become well dispersed in the resin.

Effect of the Different Ethylene Oxide Groups of Triton X Dispersants

Triton X dispersants contain different lengths of polyethylene oxide chains based on the value of *m*, and all have the same hydrophobic octylphenyl (OP) terminus, which can affect the viscosity of the silver paste and the electrical resistivity of the cured silver paste. The silver pastes were prepared by mixing 75 wt % of silver particles with 24.2 wt % of ES-100 and 0.8 wt % of various Triton X dispersants, including X-45, X-114, X-100, X-165, X-305, and X-405. The viscosities of the silver pastes are shown in Figure 5. The results indicated that the use of X-100 dispersant in preparing conductive silver paste resulted in the lowest viscosity, meaning that X-100 was the most effective at dispersing the silver particles in the polyester. This was because 9.5 PEO groups on X-100 were adsorbed on the surfaces of the silver particles in the conductive silver paste, forming a thicker, brush-like layer and generating steric hindrance among the silver particles. The greater distances between the core particles resulted in the lowest viscosity. When the silver paste contained $m < 9.5$ of X-45 and X114 dispersants, respectively, higher viscosities were produced because fewer PEO groups were adsorbed on the surfaces of the silver at same weight ratio, and insufficient steric hindrance was generated, leading to unstable suspensions. When the silver paste contained $m > 9.5$ of the dispersants (such as X165, X-304, and X-405), the viscosities also were greater because these silver pastes had excessive PEO groups, which increased the thickness of the adsorbed layers and resulted in entanglements among the excess PEO groups in the resin. Our results were consistent with those reported by Xu et al.³² who reported that excess dispersant led to higher viscosity, especially when the solid loading was high.

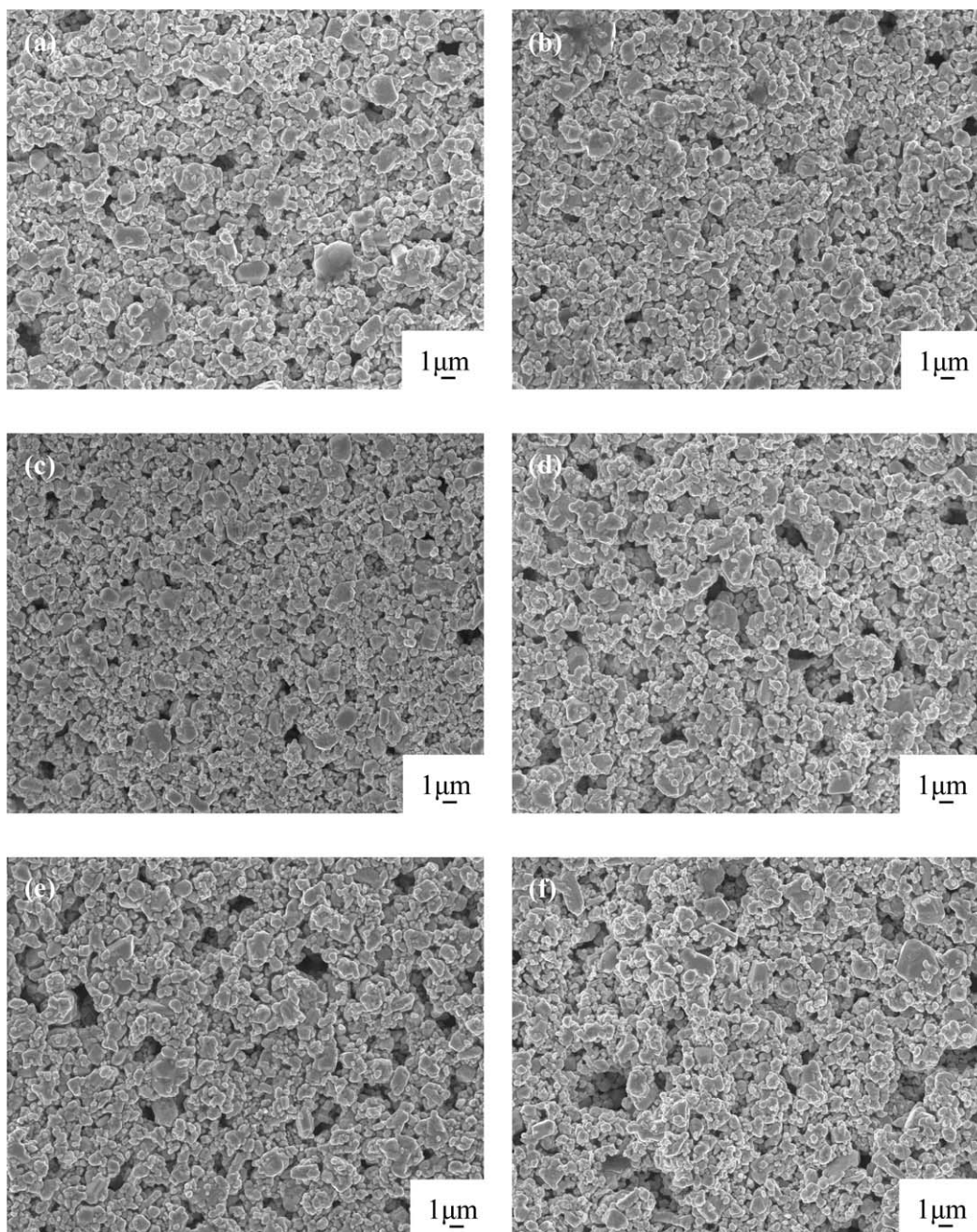


Figure 7. SEM images of 0.8 wt % of various Triton X dispersants, i.e.: (a) X-45, (b) X-114, (c) X-100, (d) X-165, (e) X-305, and (f) X-405.

Figure 6 shows the electrical resistivity of the cured silver pastes coated on the ITO film and ITO glass. Figure 6 shows that, when the cured silver pastes that had $m < 9.5$ of dispersant, such as X-45 ($m = 4.6$) and X-114 ($m = 7.5$), were coated on ITO films and ITO glass, they had the largest electrical resistivity, i.e., 8.58×10^{-5} and $9.36 \times 10^{-5} \Omega \text{ cm}$ and 7.97×10^{-5} and $6.95 \times 10^{-5} \Omega \text{ cm}$, respectively. For X-100 ($m = 9.5$), the electrical resistivities were the lowest on the ITO films and ITO glass, i.e., 5.52×10^{-5} and $6.82 \times 10^{-5} \Omega \text{ cm}$, respectively. That means the X-45 and X-114 dispersants did not do a good job of dispersing the silver particles, and their heterogeneous

distributions resulted in the cured silver pastes having greater electrical resistivities. When the cured silver pastes contained $m > 9.5$ of the dispersants, such as X-165 ($m = 16$), X-305 ($m = 30$), and X-405 ($m = 35$), the electric resistivities of the cured silver pastes increased as the value of m increased for the dispersants. Since the viscosities of the silver pastes increased as the value of m increased, the resulting poor dispersion caused the cured silver pastes to have greater electrical resistivities. In addition, the PEO groups were nonconductors, so the existence of greater numbers of PEO groups on the surfaces of the silver particles meant that there was greater resistance to the flow of

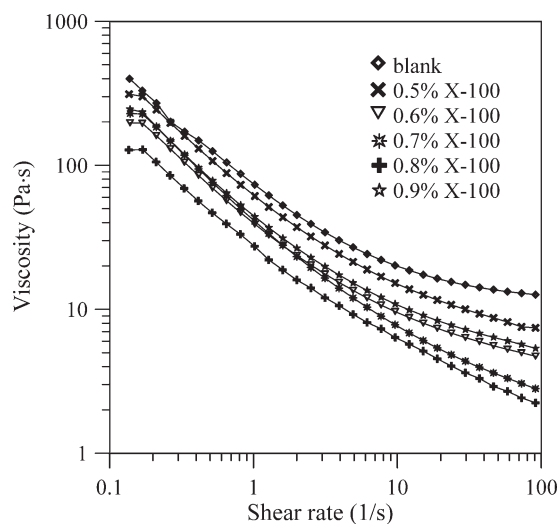


Figure 8. Viscosities of the silver pastes with different contents of the X-100 dispersant.

electricity, i.e., higher electrical resistivity. Therefore, the X-100 dispersant had a suitable amount, i.e., $m = 9.5$, which provided good dispersion properties for the silver particles, thereby decreasing the viscosity of the conductive silver paste and providing low electrical resistivity of the cured silver paste.

The voids were provided by the evaporation of the solvents and dispersants when the silver pastes were cured at 140°C . The voids that existed in the cured silver paste also were impediments to electrical conduction since all of the compositions had the same amount of solvent. Therefore, we did not consider the effect of the solvent. Figure 7 shows the SEM images of the void distributions in the cured silver pastes for various Triton X dispersants. Figure 7(a–c) show that the cured silver pastes made with X-45 and X-114 had more voids than those made with X-100 dispersant because X-100 had a higher boiling point (270°C) than X-45 (200°C) and X-114 (177°C). When the con-

ductive silver pastes were cured at 140°C , the dispersants with higher boiling points were discharged slowly from the paste, forming fewer or smaller voids in the cured silver pastes; thus, they had lower electrical resistivity. When the conductive silver pastes contained X-165, X-305, and X-405 dispersants, larger voids existed in the cured silver pastes, as shown in Figure 7(d–f). This was due to the fact that X-165, X-305, and X-405 dispersants had the same boiling point, i.e., 101°C , which was lower than the curing temperature of 140°C , so when silver paste cured, the lower boiling point dispersants were discharged rapidly from the paste, making more and larger voids, resulting in their having higher electrical resistivities.

Effect of Different Content of X-100 Dispersant

The conductive silver pastes that contained X-100 dispersant produced the cured silver pastes that had the lowest electrical resistivity. Therefore, we investigated the effects of different contents of the X-100 dispersant on the electrical resistivity of the pastes. The silver pastes were prepared by mixing 75 wt % of silver particles with different amounts of X-100, i.e., 0.5, 0.6, 0.7, 0.8, and 0.9 wt %. Figures 8 and 9 show the viscosities of the conductive silver pastes and the electrical resistivities of the cured silver pastes on ITO film and ITO glass, respectively. The results indicated that the blank paste coat on the ITO film and ITO glass resulted in the largest electrical resistivities, i.e., 9.1×10^{-5} and $1.14 \times 10^{-4} \Omega \text{ cm}$, respectively. This was because the blank had the highest viscosity, and the silver particles were easily aggregated in the conductive silver paste and produced a heterogeneous phase, as shown by the images of the top surface and the cross-sectional areas of the cured silver paste in Figure 10(a,b). In addition, Figures 8 and 9 show that both the viscosities of the silver pastes and the electrical resistivities of the cured silver paste decreased as the content of the X-100 dispersant increased below 0.8 wt %, which caused the number and sizes of voids in the cured silver pastes to decrease as shown in Figure 10(c–h). In addition, agglomerates readily formed when insufficient amounts of dispersant were added; under these

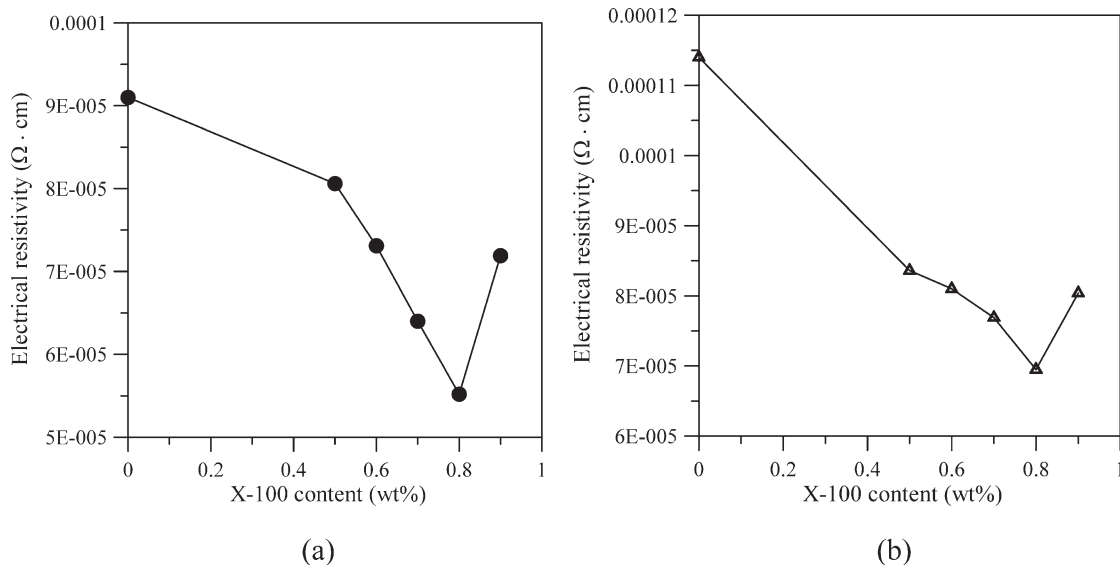


Figure 9. Electrical resistivities of the cured silver pastes with different contents of X-100 dispersant when applied to (a) ITO film; (b) ITO glass.

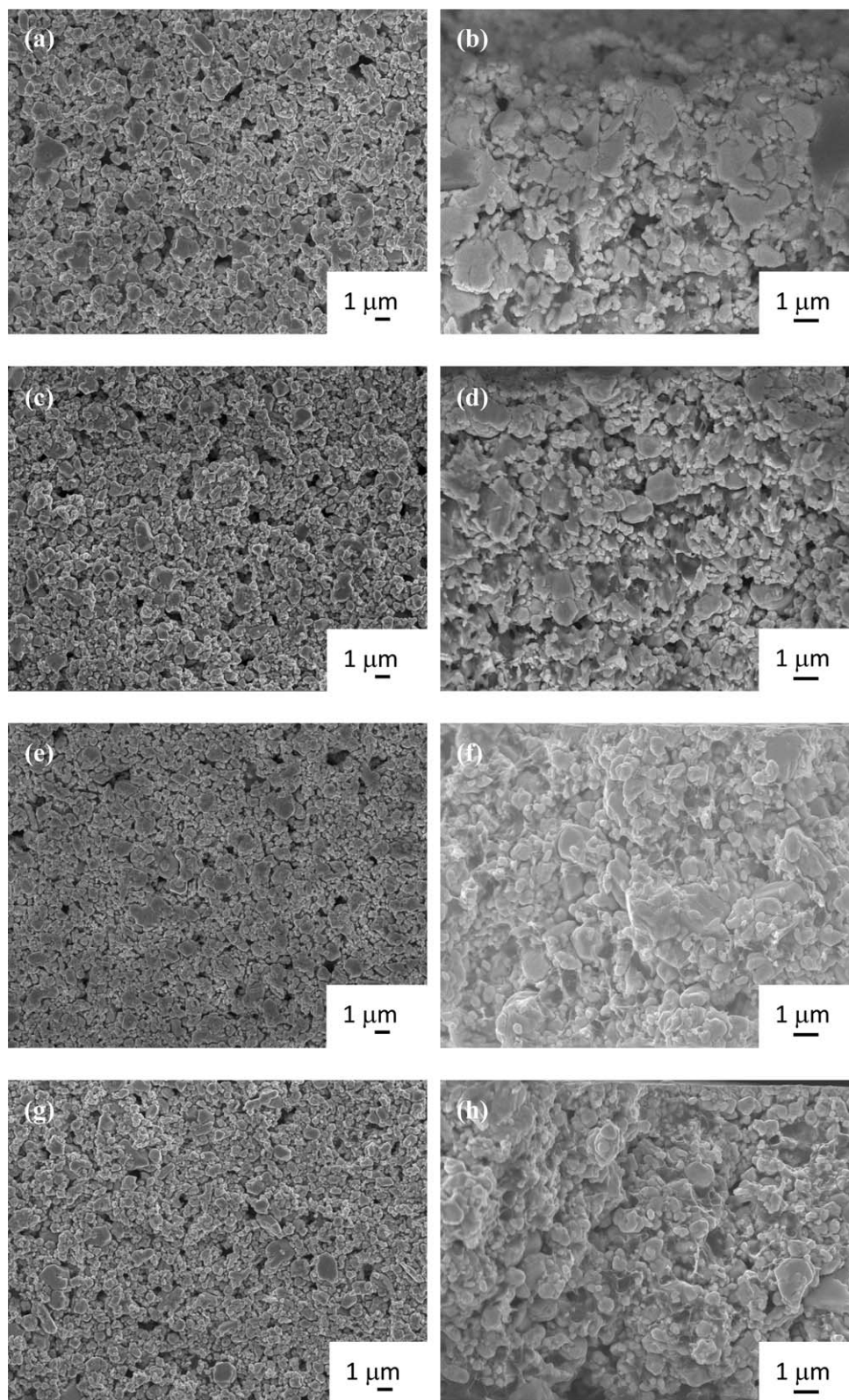


Figure 10. Top surface and cross-sectional SEM images of silver pastes with various contents of X-100 dispersants: (a) and (b) blank; (c) and (d) 0.5 wt %; (e) and (f) 0.6 wt %; (g) and (h) 0.7 wt %; (i) and (j) 0.8 wt %; (k) and (l) 0.9 wt %.

conditions, van der Waals' forces dominated the interaction between the silver particles, and the applied shear resulted in significant thinning due to the breakdown of the agglomer-

ates.³³ However, Figure 10(e,f) show that the cured microstructure of 0.6 wt % X-100 had fewer voids and larger silver grains, but some of the larger silver particles were distributed in the

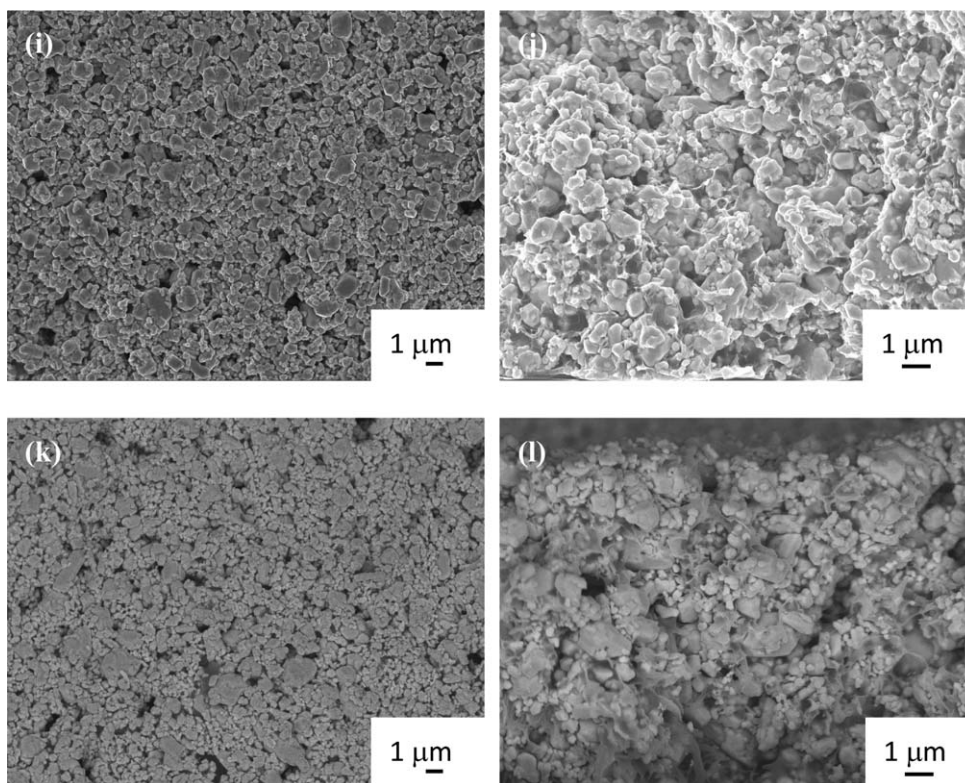


Figure 10. Continued.

middle of sample, and some of the smaller silver particles were distributed throughout the side of sample, which facilitated the flow of electricity through the nonhomogeneous form, i.e., giving it greater electrical conductivity. The silver paste that contained 0.8 wt % of the X-100 dispersant had the lowest viscosity, and Figure 10(i,j) show that less voids were formed in the cured silver paste, resulting in the lowest electrical resistivity of the two surfaces, i.e., 5.52×10^{-5} and $6.95 \times 10^{-5} \Omega \text{ cm}$, respectively. When the content of the X-100 dispersant in the conductive silver pastes was increased to 0.9 wt %, the dispersion properties were degraded, causing the conductive cured silver paste on the ITO film and ITO glass to have more voids, as shown in Figure 10(k,l), and this resulted in their having higher electrical resistivities, i.e., 7.19×10^{-5} and $8.04 \times 10^{-5} \Omega \text{ cm}$, respectively. This occurred because the conductive silver pastes that contained excess dispersant also contained excess PEO groups adsorbed on the surfaces of the silver particles, forming more entanglements that resisted the conduction of electricity.

CONCLUSIONS

In this study, the Triton X dispersants dispersed the silver particles most effectively when there was a high loading of 75 wt % of silver particles in the conductive silver paste. This was due to the fact that the molecular structures of the Triton X dispersants contained hydrophilic PEO groups that were absorbed on the hydrophilic surfaces of the silver particles through hydrophilic interaction and hydrophobic hydrocarbon groups. The hydrophobic hydrocarbon groups face the polyester as the moieties stabilize the silver particles, providing steric stabilization. When the value of m was less than 9.5, the Triton X dispersants did

not disperse the silver particles very well, causing the cured silver pastes to have higher electrical resistivities. Dispersants that had an m value greater than 9.5 allowed more PEO groups to be absorbed on the surfaces of silver particles. These groups resist the flow of electricity in the cured silver paste, thereby giving it a higher electrical resistivity. Therefore, when the number of PEO groups (m) of X-100 dispersant was 9.5, good dispersion of the silver particles occurred, decreasing the viscosity of the conductive silver paste and decreasing the electrical resistivity of the cured silver paste. For conductive silver pastes that contained 0.8 wt % or less of the X-100 dispersant, the viscosity of conductive silver paste and electrical resistivity of the cured silver paste decreased as the content of X-100 dispersant increased. When the conductive silver paste contained 0.8 wt % of the X-100 dispersant, the cured silver paste had the lowest electrical resistivity for ITO film and ITO glass, i.e., 5.52×10^{-5} and $6.82 \times 10^{-5} \Omega \text{ cm}$, respectively.

ACKNOWLEDGMENTS

The authors thank the China Steel Corporation of Taiwan for providing financial support for this research.

REFERENCES

- Dobrzański, L. A.; Muszyńska, M. *J. Appl. Mater. Manuf. Eng.* **2011**, *48*, 115.
- Shih, Y. C.; Lin, Y. H.; You, J. P.; Shi, F. G. *J. Electron. Mater.* **2013**, *42*, 410.

3. Kuramoto, M.; Ogawa, S.; Niwa, M.; Kim, K. S.; Suganuma, K. *IEEE Trans. Comp. Pack. Manuf. Technol.* **2011**, *1*, 653.
4. Lee, J. H.; Liu, D. N.; Wu, S. T. *Introduction to Flat Panel Displays*; Wiley: Chichester, **2008**; p 233.
5. Sano, S.; Katsuki, T.; Takahashi, Y.; Nakazaa, F. (Fujitsu Limited). U.S. Patent 2006/0038792A1, February 23, **2006**.
6. Kishi, H.; Mizuno, Y.; Chazono, H. *Jpn. J. Appl. Physiol.* **2003**, *42*, 1.
7. Chu, S.; Li, D.; Chang, P. C.; Lu, J. G. *Nanoscale Res. Lett.* **2011**, *6*, 1.
8. Zaman, A. *Colloid. Polym. Sci.* **2000**, *278*, 1187.
9. Reddy, S. B.; Singh, P. P.; Raghu, N.; Kumar, V. *J. Mater. Sci.* **2002**, *37*, 929.
10. Ávila, H. A.; Reboledo, M. M.; Castro, M.; Parra, R. *Mater. Res.* **2013**, *16*, 839.
11. Leng, Y. J.; Chan, S. H.; Khor, K. A.; Jiang, S. P.; Cheang, P. *J. Power Sources* **2003**, *117*, 26.
12. Kumari, V. K. G. Sasidharan, K.; Sapna, M.; Natarajan, R. *Bull. Mat. Sci.* **2005**, *28*, 103.
13. Randhawa, P.; Park, J. S.; Sharma, S.; Kumar, P.; Shin, M. S.; Sekhon, S. S. *J. Nanoelectron. Optoelectron.* **2012**, *7*, 279.
14. Xin, F.; Li, L. *J. Thermoplast. Compos. Mater.* **2013**, *26*, 227.
15. Sulong, A. B.; Muhamad, N.; Sahari, J.; Ramli, R.; Deros, B. M.; Park, J. *Eur. J. Sci. Res.* **2009**, *29*, 13.
16. Rastogi, R.; Kaushal, R.; Tripathi, S. K.; Sharma, A. L.; Kaur, I.; Bharadwaj, L. M. *J. Colloid Interface Sci.* **2008**, *328*, 421.
17. Geng, Y.; Liu, M. Y.; Li, J.; Shi, X. M.; Kim, J. K. *Compos. Part A Appl. Sci. Manuf.* **2008**, *39*, 1876.
18. Hasan, T.; Scardaci, V.; Tan, P. H.; Rozhin, A. G.; Milne, W. I.; Ferrari, A. C. *J. Phys. Chem. C* **2007**, *111*, 12594.
19. Ng, S. H.; Wang, J.; Guo, Z. P.; Chen, J.; Wang, G. X.; Liu, H. K. *Electrochim. Acta.* **2005**, *51*, 23.
20. Farahmandjou, M. *Optoelectron Adv. Mater. Rapid Commun.* **2010**, *4*, 986.
21. Zhang, J.; Ye, F.; Sun, J.; Jiang, D.; Iwasa, M. *Colloid Surf. A Physicochem. Eng. Asp.* **2005**, *254*, 199.
22. Lee, D. I.; Lee, S. M.; Lee, E. S.; Choi, J. Y.; Bae, J. Y. *J. Appl. Polym. Sci.* **2007**, *105*, 2012.
23. Kreshech, G. C.; Hwang, J. *Chem. Phys. Lipids* **1995**, *76*, 193.
24. Altschuler, M.; Heddens, D. K.; Diveley, R. R.; Krescheck, G. C. *Biotechniques* **1994**, *17*, 434.
25. Perelaer, J.; Laat de, A. W. M.; Hendriks, C. E.; Schubert, U. S. *J. Mater. Chem.* **2008**, *18*, 3209.
26. Bonnemann, H.; Richards, R. M. *Eur. J. Inorg. Chem.* **2001**, *10*, 2455.
27. Huang, J.; Xu, J.; Wang, D.; Li, L.; Guo, X. *Ind. Eng. Chem. Res.* **2013**, *52*, 8427.
28. Sui, Y.; Cui, Y.; Nie, Y.; Xia, G. M.; Sun, G. X.; Han, J. T. *Colloid Surf. B: Biointer.* **2012**, *93*, 24.
29. Shiratsuchi K.; Kubota T. (Fujifilm Corporation). U.S. Patent 2007/0196597 A1, August 23, **2007**.
30. Chen, J.; Spear, S. K.; Huddleston, J. G.; Rogers R. D. *Green. Chem.* **2005**, *7*, 64.
31. Fang, J. M.; Fowler, P.; Tomkinson, J.; Hill, C. A. S. *Carbohydr. Polym.* **2002**, *47*, 285.
32. Xu, X.; Oliveira, M. I. L. L.; Fu, R.; Ferreira, J. M. F. *J. Eur. Ceram. Soc.* **2002**, *23*, 1525.
33. Bergström, L. *Colloid Surf. A Physicochem. Eng. Asp.* **1998**, *133*, 151.